CIRP Annals - Manufacturing Technology 00 (2025) 1–5

Contents lists available at ScienceDirect

CIRP Annals - Manufacturing Technology

journal homepage: https://www.editorialmanager.com/CIRP/default.aspx

A novel method for high-volume manufacturing of self-protective plastic surfaces to ensure durable anti-counterfeiting functionality

Marco Sorgato[a], Giacomo Baruffa[a], Keltoum Oubellaouch[b,c], Giulia Zaniboni[b,c], Giovanni Lucchetta (2)[a,*]

[a] Department of Industrial Engineering, University of Padova, Padova, Italy
[b] Department of Sciences and Methods for Engineering, University of Modena and Reggio Emilia, Reggio Emilia, Italy
[c] En&Tech Interdepartmental Center, University of Modena and Reggio Emilia, Reggio Emilia, Italy

ARTICLE INFO

Article history:
Available online xxx

Keywords:
Surface modification
Injection molding
Wear

ABSTRACT

This study presents a novel approach to the high-volume manufacturing of durable self-protective polypropylene surfaces that integrate micro-scale protective grids with sub-micrometer Laser-Induced Periodic Surface Structures (LIPSS). Grids with variable pitches (40–250 μm) were designed to optimize surface durability and nanostructure functionality. Wear tests indicated that smaller grid pitches offered superior protection, significantly enhancing the functional lifespan of the structural color compared to unprotected surfaces. These findings underscore the success of optimized grid designs in delaying wear progression, providing a scalable and practical solution for durable nanostructured thermoplastic surfaces in industrial applications.

1. Introduction

Micro and nanostructured surfaces are designed to enhance functionality by modifying surface properties [1]. Their unique optical effects make them valuable in anti-counterfeiting technologies [2,3]. However, transitioning these surfaces to industrial applications is challenging due to durability and scalability issues. Hierarchical structures combining micro- and nanoscale features offer a promising solution, with microscale elements providing robustness and nanoscale features delivering advanced functionalities [4]. These "self-protective surfaces" maintain structural integrity under mechanical stresses, making them suitable for precision and durability applications [5,6]. Several studies have explored hierarchical designs. Xiu et al. demonstrated the enhanced durability of hierarchical silicon structures compared to unprotected surfaces under abrasion tests [7]. Similarly, Wang et al. developed microscale pockets to protect superhydrophobic nanostructures, maintaining their properties after wear on various substrates, including metal, glass, and ceramics [8]. Lin et al. designed a durable, water-repelling mesh by embedding carbon nanofibers into stainless steel and reinforcing it with a PDMS coating, which retained its properties after multiple abrasion cycles [9]. Groten et al. fabricated superhydrophobic surfaces with microposts and nanograss using silicon etching and a fluoropolymer coating. The hierarchical structure retained superhydrophobicity under higher loads compared to unprotected nanograss [10]. Qing et al. created a surface with durable wetting properties by fabricating a porous iron film filled with inorganic nanoparticles and an organic medium, maintaining its functionality after abrasion and impact tests [11]. Using a nanosecond laser, Boinovich et al. modified the topography and physicochemical properties of an Al-Mn alloy surface properties. The surface was proved through a two-hour abrasion test [12].

These methods often rely on complex and costly processes or materials with high mechanical strength, which are unsuitable for large-scale production. In contrast, thermoplastics are cost-effective and suitable for high-volume replication [13–14], but they are prone to wear under mechanical stress, limiting long-term performance [15]. Addressing these challenges requires innovations in surface resilience and scalable manufacturing approaches, which could enable broader application of self-protective structures in mass production [16].

This study proposes and validates a new approach to developing self-protective nanostructured surfaces on thermoplastics, leveraging and optimizing scalable techniques such as laser structuring and injection molding. Despite its vulnerability to wear, polypropylene was chosen to investigate the potential of a commodity plastic for sustaining structural color (a crucial function for anti-counterfeiting) under mechanical stress [17–19]. Structural color was generated through LIPSS, periodic nanopatterns that form on a material's surface upon exposure to specific laser irradiation. Protective grid patterns were optimized to balance durability with structural color functionality, ensuring scalability for industrial production. Wear tests were designed and optimized to simulate real-world interactions, providing a comprehensive understanding of the surfaces' durability.

* Corresponding author.
E-mail address: giovanni.lucchetta@unipd.it (G. Lucchetta).

https://doi.org/10.1016/j.cirp.2025.04.011

2. Materials and methods

2.1. Sample design and manufacturing

The design of the reinforcing microstructure was established before fabrication to address mechanical and production constraints. The protective walls were defined based on the laser beam dimensions, resulting in a triangular cross-section with a base width of 10 μm, a height of 2.5 μm, and a draft angle of 60° This geometry streamline laser processing and minimizes defects.

To evaluate the deformation behavior of the abrasive medium (PDMS) under uniform pressure, various geometric patterns were assessed, including circular, square, hexagonal, and triangular. The effect of grid pitch on PDMS deformation was modeled by treating it as a supported beam subjected to a uniform load of 0.7 MPa.

The mold inserts, made from 16MnCr5 steel and polished to a surface roughness (Sa) below 0.03 μm, were laser-textured using an EKSPLA Atlantic 50 picosecond laser system, operating at both 532 nm and 1064 nm wavelengths. Grooves were arranged in a square grid pattern with pitches of 25, 40, 50, 100, 150, 250, and 500 μm (Fig. 1a), created using the 532 nm wavelength at 75 mW power, 1200 mm/s scan speed, 400 kHz frequency, and 80 passes. The low power and high pass count ensured the desired groove depth, high surface quality, and minimal thermal impact on adjacent areas [20]. LIPSS were subsequently generated within the groove regions using the 1064 nm wavelength at 0.69 W power, 1500 mm/s scan speed, and 333 kHz frequency, oriented at 45° relative to the grid pattern (Fig. 1b) [21]. Unprotected inserts (UP), which lacked reinforcing walls, were also fabricated for comparison. All inserts featured an inverted L-shaped reference to ensure accurate alignment during subsequent measurements.

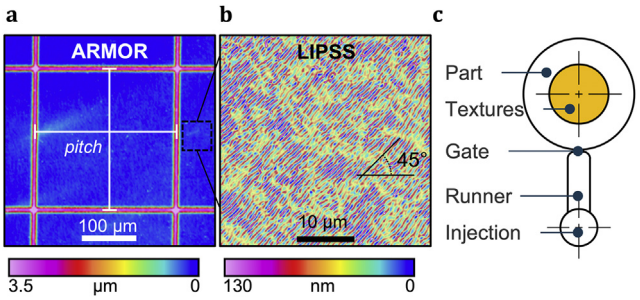

Fig. 1. Sample geometry: (a) micro-scale protective armor; (b) nano-scale LIPSS; (c) schematization of the molded part.

The inserts were used to replicate polypropylene discs with a diameter of 18 mm and a thickness of 2 mm (Fig. 1c) through micro-injection molding (Micropower 15, Wittmann-Battenfeld). Process parameters were optimized to ensure high-fidelity replication of both the micro- and nanofeatures.

2.2. Wear tests

The replicated samples were tested for wear resistance using a tribometer (MFT-5000, Rtec-Instruments). The setup consisted of sliding a PDMS pin across the sample surfaces. A 5:1 PDMS mixture (5 parts catalyst) with an elastic modulus of 13 MPa was used as the abrasive medium to simulate human touch. Precise alignment of the microgrid with the wear direction (the pin travels at 45° with respect to the x-axis shown in Fig. 2a) was ensured. A vertical force (F) of 7 N was applied, and the sample was moved at 25 mm/s over a 6 mm stroke (L) for a specified duration [22].

Wear tests were conducted at 0 to 90 min intervals, with measurements taken every 15 min to monitor wear progression. It is worth noting that the applied test pressure of 0.7 MPa significantly exceeds the pressure typically generated by hand contact, which ranges between 0.01 and 0.1 MPa. As a result, the testing conditions were intentionally accelerated to evaluate the durability of the surfaces within a shorter timeframe. Given the abrasive nature of the wear

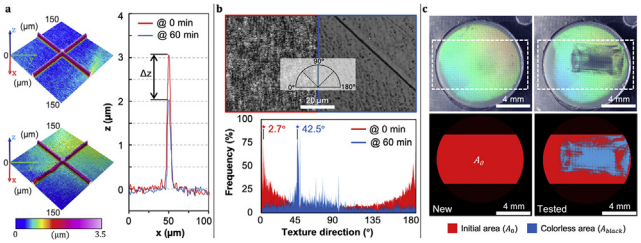

Fig. 2. Part characterization procedure: (a) grid walls height measurements; (b) nanostructures directionality evaluation; (c) and determination of the structured color evolution.

mechanism, Archard's law (Eq. (1)) was applied to verify the durability of the LIPSS under realistic loads:

$$V = k\frac{FLn}{H} \tag{1}$$

where V is the volume of material removed due to wear, k is the wear coefficient, n the number of the wear cycles and H is the polypropylene hardness. The wear coefficient k was obtained by fitting Archard's law to wall volume variations, with fittings repeated for all reinforcement pitches to account for microstructural effects on PP-PDMS contact.

2.3. Surface characterization

The mold inserts and replicated samples were characterized to verify the replication quality and to evaluate the wear evolution [23,24]. A confocal profilometer (PluS Neox, Sensofar) equipped with a 100 × objective was used to scan a 0.87 × 0.98 mm^2 area (stitching of 7 × 8 areas was performed with a 25 % overlap) at the center of the nanostructured area. The reference marker on the inserts ensured consistent scan positioning. The geometry of the microfeatures (armor) was analyzed on three polymeric samples for each insert. The micro-level replication was evaluated by comparing the average height of the replicated micro-walls on the plastic samples $\overline{h}_{wall}$ and the average depth of the micro-walls on the mold insert $\overline{w}_{wall}$(Eq. (2)):

$$Q_{micro} = \frac{\overline{h}_{wall}}{\overline{w}_{wall}} \cdot 100 \tag{2}$$

Roughness analyses were carried out on the mold inserts and the molded parts according to the EN ISO 25,178−3 standard (S-L filter was used, applying λ_s = 300:1 and λ_L = 0.0025 mm). To assess the replication quality during the molding process, the average *Spk* (reduced peak height) and *Svk* (reduced valley depth) values measured on the mold inserts were directly compared with the corresponding average *Svk* and *Spk* values from the molded parts, obtaining the replication indexes Q_v and Q_p (Eq. (3) and 4):

$$Q_v = \frac{Svk_{molded\ part}}{Spk_{mold\ insert}} \cdot 100 \tag{3}$$

$$Q_p = \frac{Spk_{molded\ part}}{Svk_{mold\ insert}} \cdot 100 \tag{4}$$

To evaluate the wear evolution and apply Archard law (Eq. (1)), all molded components were characterized with a focus on three aspects: i) the height variation of the protective microstructure walls, ii) changes in the directionality of the nanostructures, and iii) the evolution of the structured color (Fig. 2).

The variation in the height of the protective walls was analyzed using confocal profilometry scans, providing measurements of material loss due to wear (V in Eq. (1), Fig. 2a). For the nanoscale evaluation, the directionality of the nanostructures was monitored. Since LIPSS are inherently aligned in a specific direction, wear applied at a 45° angle introduced grooves that disrupted their original alignment, resulting in a measurable change in their directionality (Fig. 2b). The evaluation of structural color evolution under wear conditions was limited to inserts with grid pitches of 40, 100, and 250 μm. These

Please cite this article as: M. Sorgato et al., A novel method for high-volume manufacturing of self-protective plastic surfaces to ensure durable anti-counterfeiting functionality, CIRP Annals - Manufacturing Technology (2025), https://doi.org/10.1016/j.cirp.2025.04.011

configurations ensured the functionality of LIPSS-based structural color and provided a range for analysis [25,26]. Pitches below 40 μm compromised structural color due to wall interference, while pitches over 250 μm were excluded as larger spacing allowed direct PDMS contact with LIPSS from the start of wear, as explained in the Results section. The structural color analysis was performed using a Keyence (VHX-S770E/S750E with a VHX-E20 objective) optical microscope. Images at 20 × magnification were converted into topographical surfaces based on the colors detected in the image, using the software MountainsMap. A threshold-based analysis was then applied to isolate and quantify areas where structural color was lost due to wear (Fig. 2c). The colorless area (A_{black}) was expressed as a percentage of the initial area (A_0), corresponding to the region traversed by the PDMS pin during the wear tests.

To ensure statistical robustness, all parameters were measured on five samples, with roughness and height assessed in six areas per sample. Variability is expressed as the standard deviation.

3. Results and discussion

3.1. Grid design

The surface design was guided by grid shape and pitch, as a denser grid improves durability but reduces the area available for nanostructures, requiring an optimal balance between protection and functionality. As shown in Fig. 3a, square and hexagonal grids maximize the area available for nanostructures and were prioritized for further investigation. The effect of grid pitch on PDMS deformation is presented in Fig. 3b

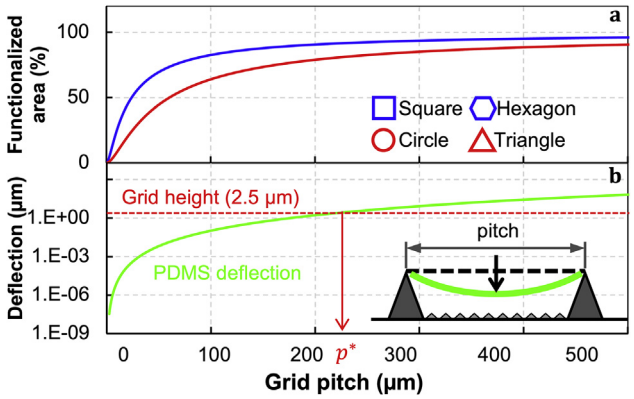

Fig. 3. Results of the design phase: (a) effect of grid shape on functionalized area; (b) effect grid pitch on PDMS deflection.

Grid pitches below 220 µm effectively limit PDMS deflection to heights below the grid walls (p^* in Fig. 3b), preventing premature contact with the nanostructures. This ensures the grid acts as a sacrificial layer, protecting the underlying surface and preserving nanostructure functionality.

3.2. Mold manufacturing and micro-injection molding

Table 1 reports the micro- and nano-replication indexes. At the micro level, replication efficiency (Q_{micro}) consistently exceeded 92 %, indicating that polypropylene replicates the walls well. As the grid pitch decreases, replicating the nanostructure with the same level of accuracy becomes progressively more challenging (Q_v,Q_p). This phenomenon is primarily attributed to the hesitation effect, which occurs when a polymer flow is temporarily delayed upon encountering regions of varying geometry [27,28]. After the polymer fills the microcavity, it flows into the micro-structured regions to replicate the walls and only subsequently reaches the sub-micrometer features (LIPSS). The closely spaced micro-walls create narrower flow paths and increase localized resistance, further hindering the effective replication of nanostructures. Despite these issues, the level of replication of nanofeatures is considered sufficient for the purposes of this work.

Table 1
Part replication indexes

Grid pitch (μm)	Q_{micro} (%)	Q_v (%)	Q_p (%)
25	93.7 ± 0.3	73.4 ± 4.8	70.1 ± 1.7
40	94.7 ± 2.0	87.5 ± 0.4	86.5 ± 5.1
50	92.8 ± 0.4	87.2 ± 1.8	80.5 ± 0.9
100	95.2 ± 1.0	95.6 ± 4.6	94.4 ± 3.6
150	98.1 ± 1.6	94.6 ± 4.8	93.7 ± 5.1
250	96.7 ± 0.8	98.5 ± 4.9	98.1 ± 1.8
500	96.1 ± 0.3	97.1 ± 6.1	97.1 ± 5.8
UP	/	97.3 ± 0.9	98.1 ± 2.9

3.3. Nanostructure durability

The durability of the LIPSS was evaluated through wear tests (Fig. 4a) using two metrics: wear onset, marking the initial deviation of the primary texture (aligned with the x-axis, parallel to the LIPSS), and where the wear-induced directionality (at 45°) dominates. The micrograph in Fig. 4b shows that LIPSS displays evident degradation after testing, with residual LIPSS interspersed with wear grooves from the PDMS pin's repeated passages. The nanostructure durability results are summarized in Fig. 5. For microgrid patterns, the failure mechanism is progressive. Initially, protective walls absorb wear, preventing direct PDMS contact with the LIPSS. This stability reflects a narrow variability in primary texture directionality, showing strong resistance to early wear. A transitional phase occurs as testing continues, marked by increased texture directionality standard deviation, indicating gradual wall degradation until PDMS contacts the nanostructures. The directionality stabilizes at 45° as wear grooves dominate and LIPSS degrade completely. Unprotected patterns exhibit an abrupt failure mechanism. LIPSS contacts PDMS from the onset of wear without protective walls, rapidly increasing the surface texture directionality's standard deviation. Wear grooves form quickly, highlighting unreinforced samples' inability to withstand early wear. Fig. 5 further illustrates the relationship between grid pitch and surface durability. Samples with a pitch of 25 μm exhibit the highest durability, as the protective walls effectively delay direct PDMS contact with the LIPSS, mitigating wear progression. In contrast, grids with a 500 μm pitch offer minimal protection due to the wide spacing, resulting in early wear onset and rapid stabilization of the surface texture directionality at 45° [10,29].

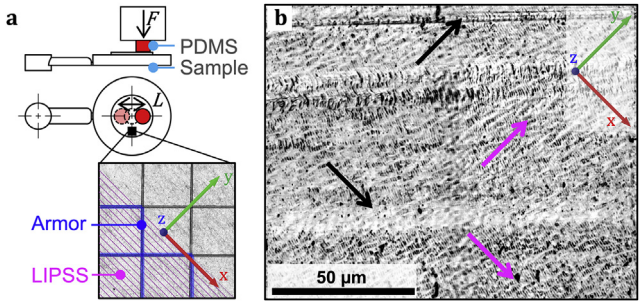

Fig. 4. Wear test: (a) schematization of setup and coordinate system; (b) worn PP sample showing wear grooves (black) and lasting LIPSS (pink).

Intermediate pitches, such as 250 μm, approach a critical threshold at which the grid offers only partial protection. In this case, the failure mechanism is not as straightforward, likely resulting from a combination of PDMS deformation, wall deformation, and the limited resolution of the sampling intervals. No significant differences occurred for 40, 50, 100, and 150 μm pitches, stabilizing around 30 min. This uniformity masks subtle variations in the durability of these grid configurations due to the discrete sampling process. The lifetime of each sample was defined as the step immediately before wear onset. For example, the lifetime of the

Please cite this article as: M. Sorgato et al., A novel method for high-volume manufacturing of self-protective plastic surfaces to ensure durable anti-counterfeiting functionality, CIRP Annals - Manufacturing Technology (2025), https://doi.org/10.1016/j.cirp.2025.04.011

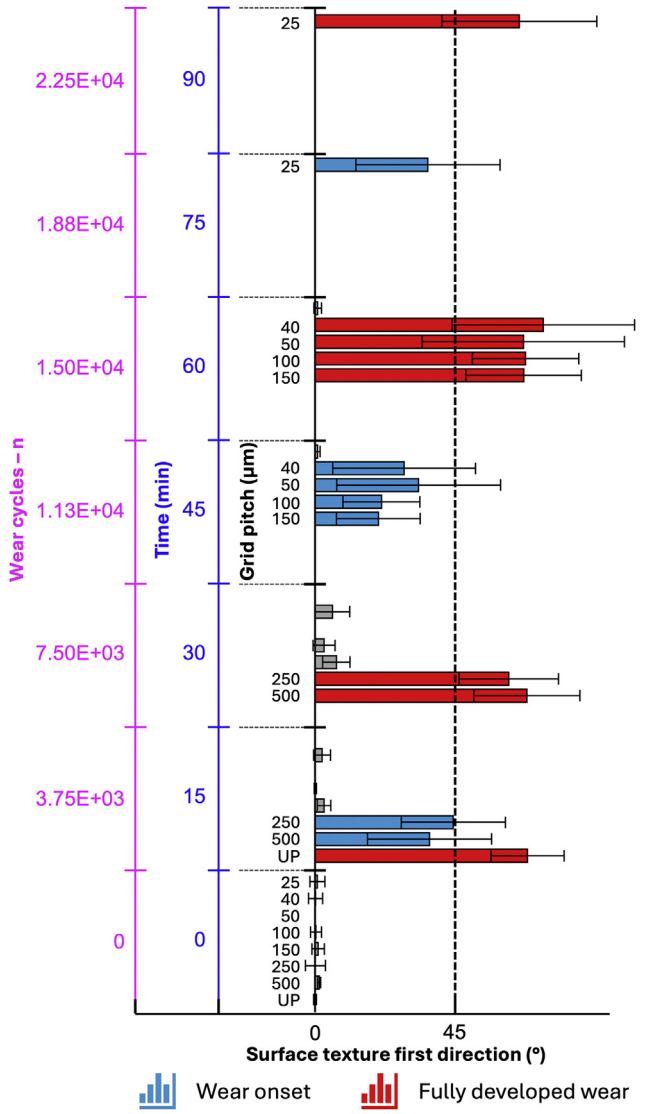

Fig. 5. Nanostructures durability results based on texture first direction.

grid with a 100 μm pitch was 7.5 $\times$ 10^3 cycles, as wear onset occurred at 1.13 $\times$ 10^4 cycles.

3.4. Functionality evaluation

Fig. 6 illustrates the progression of the colorless area (A_{black}/A_0) over time for the tested samples (unprotected - UP, 40 μm, 100 μm, 250 μm). A_{black} quantifies the dimension of the region lacking structural coloration, corresponding to the black areas visible in Fig. 6 (sampled according to Section 2.3). A 30-minute test duration was chosen based on prior findings, as wear onset occurs at this time for samples with grid pitches of 40 μm and 100 μm.

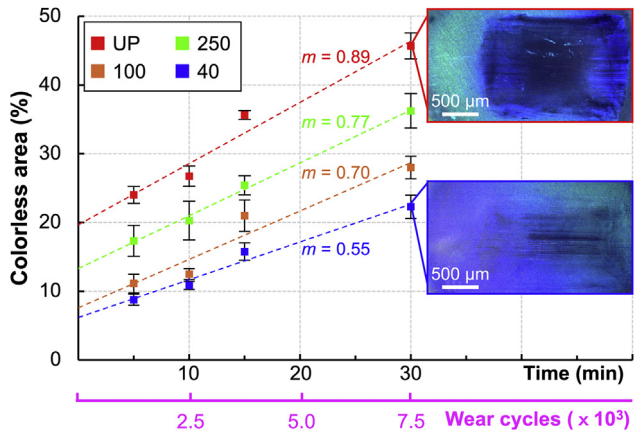

Fig. 6. Evolution of the colorless ratio over time and corresponding wear cycles.

At t = 0, all samples exhibit similar coloration, confirmed by RGB spectral measurements at three points per sample, with color variation consistently below 5 %. This indicates the protective grid does not impair the surface's initial functionality.

Linear regression analysis revealed a minimum R^2 value of 0.93, confirming the reliability of the results. For UP samples, the colorless area increases from 22 % after 5 min to 46 % after 30 min, with a color-loss ratio (slope m in Fig. 6) of 0.89. Conversely, samples with higher grid densities, such as 40 μm grids, exhibited significantly lower color-loss ratios and smaller colorless areas, confirming the effectiveness of self-protective structures in delaying wear. The reduction in nanofeature height diminishes color intensity even when LIPSS are not fully worn out [30,31].

The behavior of self-protective surfaces under hand contact conditions was predicted using Archard's law. Fig. 6 was used to determine the time (and consequently the wear distance) at which color loss becomes excessive under accelerated test conditions, potentially compromising the anti-counterfeiting functionality. The threshold value is application-dependent. In the following example, a cut-off value of 20 % was selected for the colorless area. The wear coefficient k was fitted as described in Section 2.2. Finally, the predicted surface lifespans were calculated by imposing an equivalent volume loss between the two loading conditions. Specifically, the 40 μm grid exhibited an estimated duration of 4.38 $\times$ 10^5 cycles, compared to 8.75 $\times$ 10^3 cycles for the UP surface. This substantial increase underscores the grid's effectiveness in mitigating wear progression and maintaining LIPSS functionality under realistic operating conditions.

4. Conclusions

This study demonstrates that integrating micro-scale protective grids with LIPSS significantly enhances the durability of functional polypropylene surfaces under abrasive wear conditions. The results show that a 40 μm grid pitch effectively delays wear progression, preserving the structural color functionality for up to 4.38 $\times$ 10^5 cycles under realistic loading conditions.

These self-protective surfaces offer promising applications in fields requiring enhanced surface durability and functionality, including anti-counterfeiting technologies, where structural color provides a tamper-resistant visual signature. In conclusion, this research advances the design of durable hierarchical surfaces and validates a novel method for high-volume manufacturing of self-protective plastic surfaces that ensure durable anti-counterfeiting functionality.

Declaration of competing interest

The authors declare that they have no known competing financial interests or personal relationships that could have appeared to influence the work reported in this paper.

CRediT authorship contribution statement

Marco Sorgato: Writing – review & editing, Writing – original draft, Visualization, Validation, Methodology, Formal analysis, Data curation, Conceptualization. **Giacomo Baruffa:** Writing – review & editing, Writing – original draft, Methodology, Investigation, Formal analysis, Conceptualization. **Keltoum Oubellaouch:** Writing – review & editing, Investigation, Conceptualization. **Giulia Zaniboni:** Writing – review & editing, Investigation, Conceptualization. **Giovanni Lucchetta:** Writing – review & editing, Supervision, Project administration, Funding acquisition, Conceptualization.

Please cite this article as: M. Sorgato et al., A novel method for high-volume manufacturing of self-protective plastic surfaces to ensure durable anti-counterfeiting functionality, CIRP Annals - Manufacturing Technology (2025), https://doi.org/10.1016/j.cirp.2025.04.011

References

[1] Fang FZ, Zhang XD, Gao W, Guo YB, Byrne G, Hansen HN (2017) Nanomanufacturing—Perspective and applications. *CIRP Annals* 66/2:683–705.
[2] Malshe AP, Bapat S, Rajurkar KP, Haitjema H (2018) Bio-inspired textures for functional applications. *CIRP Annals* 67/2:627–650.
[3] Sun Z, To S, Jiao J, Yip W, Wang S, Wu H (2024) High-frequency diamond imprinting of fine-crystallized micro-structured surfaces. *CIRP Annals* 73/1:429–432.
[4] Brinksmeier E, Karpuschewski B, Yan J, Schönemann L (2020) Manufacturing of multiscale structured surfaces. *CIRP Annals* 69/2:717–739.
[5] Zimmermann J, Reifler FA, Fortunato G, Gerhardt LC, Seeger S (2008) A simple, one-step approach to durable and robust superhydrophobic textiles. *Adv Funct Mater* 18/22:3662–3669.
[6] Zhang W, Wang D, Sun Z, Song J, Deng X (2021) Robust superhydrophobicity: mechanisms and strategies. *Chem Soc Rev* 50/6:4031–4061.
[7] Xiu Y, Liu Y, Hess DW, Wong CP (2010) Mechanically robust superhydrophobicity on hierarchically structured Si surfaces. *Nanotechnology* 21:155705.
[8] Wang D, Sun Q, Hokkanen MJ, Zhang C, Lin FY, Liu Q, Deng X (2020) Design of robust superhydrophobic surfaces. *Nature* 582:55–59.
[9] Lin X, Heo J, Jeong H, Choi M, Chang M, Hong J (2016) Robust superhydrophobic carbon nanofiber network inlay-gated mesh for water-in-oil emulsion separation with high flux. *Journal of Materials Chemistry A* 4:17970–17980.
[10] Groten J, Rühe J (2013) Surfaces with combined microscale and nanoscale structures: a route to mechanically stable superhydrophobic surfaces? *Langmuir* 29/11:3765–3772.
[11] Qing Y, Shi S, Lv C, Zheng Q (2020) Microskeleton-nanofiller composite with mechanical super-robust superhydrophobicity against abrasion and impact. *Adv Funct Mater* 30/39:1910665.
[12] Boinovich LB, Modin EB, Sayfutdinova AR, Emelyanenko KA, Vasiliev AL, Emelyanenko AM (2017) Combination of functional nanoengineering and nanosecond laser texturing for design of superhydrophobic aluminum alloy with exceptional mechanical and chemical properties. *ACS nano* 11/10:10113–10123.
[13] Holthusen AK, Riemer O, Schmütz J, Meier A (2017) Mold machining and injection molding of diffractive microstructures. *J Manuf Process* 26:290–294.
[14] Li D, Zhang Y, Liu Y, Regi F, Doest MEB, Tosello G (2022) Injection moulding of mechanical micro-manufactured structures for optically encoding plastic surfaces. *Opt Mater* 123:111822.
[15] Romano JM, Gulcur M, Garcia-Giron A, Martinez-Solanas E, Whiteside BR, Dimov SS (2019) Mechanical durability of hydrophobic surfaces fabricated by injection moulding of laser-induced textures. *Appl Surf Sci* 476:850–860.
[16] Chen F, Wang Y, Tian Y, Zhang D, Song J, Crick CR, Lu Y (2022) Robust and durable liquid-repellent surfaces. *Chem Soc Rev* 51/20:8476–8583.
[17] Teutoburg-Weiss S, Soldera M, Bouchard F, Kreß J, Vaynzof Y, Lasagni AF (2022) Structural colors with embedded anti-counterfeit features fabricated by laser-based methods. *Optics & Laser Technology* 151:108012.
[18] Guo P, Yang Y (2019) A novel realization of diffractive optically variable devices using ultrasonic modulation cutting. *CIRP Annals* 68/1:575–578.
[19] Qian, J., & Zhao, Q.Z., 2020, Anti-counterfeiting microstructures induced by ultrashort laser pulses, physica status solidi (a), 217/11, 1901052.
[20] Orazi L, Romoli L, Schmidt M, Li L (2021) Ultrafast laser manufacturing: from physics to industrial applications. *CIRP Annals* 70/2:543–566.
[21] Florian C, Kirner SV, Krüger J, Bonse J (2020) Surface functionalization by laser-induced periodic surface structures. *J Laser Appl* 32/2.
[22] Myshkin NK, Pesetskii SS, Grigoriev AY (2015) Polymer tribology: current state and applications. *Tribology in Industry* 37/3:284.
[23] Hansen HN, Hocken RJ, Tosello G (2011) Replication of micro and nano surface geometries. *CIRP Annals* 60/2:695–714.
[24] Jiang X, Senin N, Scott PJ, Blateyron F (2021) Feature-based characterisation of surface topography and its application. *CIRP Annals* 70/2:681–702.
[25] Jwad T, Penchev P, Nasrollahi V, Dimov S (2018) Laser induced ripples' gratings with angular periodicity for fabrication of diffraction holograms. *Appl Surf Sci* 453:449–456.
[26] Yao J, Zhang C, Liu H, Dai Q, Wu L, Lan S, Lysak TM (2012) Selective appearance of several laser-induced periodic surface structure patterns on a metal surface using structural colors produced by femtosecond laser pulses. *Appl Surf Sci* 258/19:7625–7632.
[27] Lucchetta G, Sorgato M, Carmignato S, Savio E (2014) Investigating the technological limits of micro-injection molding in replicating high aspect ratio micro-structured surfaces. *CIRP Annals* 63/1:521–524.
[28] Sorgato M, Bornillo K, Lucchetta G (2024) Reducing rubber-plastic friction in syringes through microstructured surface design and manufacturing. *CIRP Annals*.
[29] Kondrashov V, Rühe J (2014) Microcones and nanograss: toward mechanically robust superhydrophobic surfaces. *Langmuir* 30/15:4342–4350.
[30] Quan YJ, Kim MS, Kim Y, Ahn SH (2019) Colour-tunable 50 % strain sensor using surface-nanopatterning of soft materials via nanoimprinting with focused ion beam milling process. *CIRP Annals* 68/1:595–598.
[31] Yang Y, Guo P (2018) Effect of elliptical vibration trajectories on grating structure formation and its application in structural coloration. *Procedia Manufacturing* 26:543–551.

Please cite this article as: M. Sorgato et al., A novel method for high-volume manufacturing of self-protective plastic surfaces to ensure durable anti-counterfeiting functionality, CIRP Annals - Manufacturing Technology (2025), https://doi.org/10.1016/j.cirp.2025.04.011